

A Robot Model for Detecting Smoking Violations Using YOLOv5 and PID-Based Navigation Control

¹Selamat Muslimin, ^{2*}Muhammad Andaru Megaarta, ³Rayhan Triandika

^{1,2,3}Department of Electrical Engineering, Politeknik Negeri Sriwijaya, Indonesia

Email: ¹selamet_muslimin@polsri.ac.id, ²andarumega05@gmail.com, ³rayhan.triandika64@gmail.com

Article Info

Article history:

Received May 31th, 2025

Revised Jun 27th, 2025

Accepted Jul 30th, 2025

Keyword:

Autonomous Robot

Object Detection

PID

Smoking Violation

YOLOv5

ABSTRACT

Smoking violations in restricted areas, especially in public spaces exposed to secondhand smoke, remain a significant concern. This study develops an autonomous robot designed to detect smoking violations using YOLOv5 and Raspberry Pi. The robot's camera captures real-time images to identify smoking behavior, with YOLOv5 accurately detecting cigarette objects. For navigation, the robot employs a PID control system, complemented by an encoder and a compass sensor, ensuring precise movement. The results demonstrate that the robot achieves a confidence level of 87% in detecting smoking behavior at a distance of 250 cm, with a frame rate of 8 FPS. The PID-based navigation system ensures minimal error of ± 5 cm over a 2-meter distance. These findings emphasize the robot's effectiveness in both detecting smoking violations and navigating accurately, making it an effective tool for the enforcement of smoke-free zone regulations

Copyright © 2025 Puzzle Research Data Technology

Corresponding Author:

Muhammad Andaru Megaarta,

Departement of Electrical Engineering,

Politeknik Negeri Sriwijaya,

Jl. Srijaya Negara, Bukit Besar Palembang, South Sumatra, 30139.

Email: andarumega05@gmail.com

DOI: <http://dx.doi.org/10.24014/ijaidm.v8i2.37345>

1. INTRODUCTION

The ban on smoking in public places plays a crucial role in protecting public health. According to the World Health Organization (WHO), tobacco smoke causes over 8 million deaths worldwide each year. A significant portion of these deaths result from exposure to secondhand smoke in public areas. In Indonesia, about 75.5% of people are exposed to tobacco smoke in enclosed spaces, and 67.2% encounter it in public places [1]. Indonesia has established Smoke-Free Zone (SFZ) policies to protect public spaces from exposure to tobacco smoke. However, implementation faces persistent challenges, including low public compliance, inconsistent enforcement, and insufficient monitoring systems. These gaps have allowed detectable nicotine levels in designated non-smoking areas, particularly restaurants and entertainment venues, undermining the policy's health protection goals [2].

Manual monitoring of smoking violations remains vital for enforcing public health regulations, but its labor-intensive nature and reliance on human resources pose significant operational challenges. Although it remains important to enforce the rules effectively. However, Manual methods like patrols have limitations when it comes to accurately detecting specific behaviors such as smoking [3]. This is where technology can play a valuable role. With the rapid progress in sensing and detection technologies, automated solutions have become the preferred choice [4].

The increasing deployment of robots across diverse sectors has accelerated research and innovation in robotic design and control systems. Among the various categories, mobile robots have emerged as a critical focus due to their capability to operate autonomously in dynamic environments. These robots are widely employed in industrial applications and daily life, particularly for logistics and material handling tasks that demand precise navigation to designated locations. One of the fundamental components in mobile robot operation is the navigation system [5]. In the context of monitoring smoking violations, object detection

technology plays a crucial role. This technology allows robots to identify and locate specific objects in their surroundings, such as cigarettes, thereby enhancing the effectiveness of surveillance and enforcement efforts.

One of the most widely used for object detection is YOLO (You Only Look Once). YOLO is a highly efficient deep learning algorithm that detects objects in images or videos in a single pass, enabling real-time performance. Unlike traditional methods that process images multiple times, YOLO divides an image into a grid and simultaneously predicts bounding boxes and class probabilities, making it both fast and accurate for various applications [6].

Previous research on smoking detection was conducted by Madabhushi Aditya et al. (2023) [7] under the title "Smoking Detection using Deep Learning." This study utilized a balanced dataset of 7,000 images evenly divided between smokers and non-smokers. The proposed method achieved a classification accuracy of 96.74%, with a recall of 96% and a precision of 95.05%. To enhance the detection of small objects such as cigarettes, the approach combined Feature Pyramid Networks (FPN) with dilated convolution techniques. Furthermore, the study introduced an optimized YOLOv5-based model, termed Dec-YOLOv5, which employs network decomposition to reduce computational load by up to 80% without compromising accuracy. These advancements demonstrate significant improvements in both efficiency and effectiveness for real-time smoking behavior detection.

In their study titled "Region Extraction Based Approach for Cigarette Usage Classification Using Deep Learning", Pundhir et al [8]. proposed a hybrid framework combining YOLO-v3 for face-hand region extraction with transfer learning on ResNet-50. The model was trained on a balanced dataset of 2,400 images captured across diverse environmental conditions. Evaluation results demonstrated robust performance, achieving a classification accuracy of 96.74%, with complementary metrics of 96% recall and 95.05% precision.

In a study conducted by Ilham Sayekti (2022) [9], a wheeled robot navigation system was developed using a compass sensor in combination with a rotary encoder to accurately detect the robot's orientation during movement. The relationship between encoder-based odometry and compass measurements was analyzed using the linear equation $y = 0.995x - 1.553$. Experimental results demonstrated an average orientation error of 2.3° , with a maximum error of 4.2° over a travel distance of 10 meters. These findings highlight the necessity for dynamic calibration techniques to maintain accuracy in long-range navigation applications.

To enhance the effectiveness of smoke-free zone (SFZ) enforcement, there is a pressing need for improved monitoring systems that leverage advanced technologies. Autonomous robots capable of directly detecting smoking behavior represent a promising solution. This technology facilitates automatic identification and surveillance of violations, enabling more accurate and efficient enforcement of regulations. Ultimately, such innovations contribute to creating healthier and safer public environments by ensuring greater compliance with smoke-free policies.

2. METHOD

2.1 Route Planning Via Waypoint

The integration of waypoint-based path planning with Proportional-Integral-Derivative (PID) control has emerged as a robust methodology for autonomous robot navigation. This approach combines structured route planning with real-time error correction, enabling precise movement in dynamic environments [10]. PID control is a feedback algorithm used to correct errors between the setpoint (target) value and the actual value of a system.

$$u(t) = K_p e(t) + K_i \int_0^t e(\tau) d\tau + K_d \frac{de(t)}{dt} \quad (1)$$

Encoders are used to measure the distance travelled and speed of the wheels by counting the pulses generated from the rotation of the motor [11]. The encoder data provides feedback to the PID about the actual position of the robot, so that the PID can calculate:

1. Position error: $e_{\text{position}} = \text{target distance} - \text{actual distance}$
2. Speed error: The difference between the target speed and the actual speed.

The encoder on this robot has a resolution of 30 pulses/rotation and an accuracy of ± 0.5 cm at a distance of 2 metres. This data enables the robot to navigate along the specified path and compensate for drift caused by wheel friction or uneven terrain. The compass sensor on this robot detects the robot's heading ($0^\circ - 360^\circ$) relative to the Earth's magnetic field [12]. This sensor is used for:

1. Calculating error direction: $e_{\text{direction}} = \text{target heading} - \text{heading aktual}$
2. Correct directional deviation by adjusting the speed of the left/right motor.

The compass sensor is calibrated in an area free from magnetic interference, resulting in a measurement error of $\pm 2^\circ$. The compass data is combined with an encoder to calculate the robot's relative position, ensuring accurate navigation even in dynamic environments. PID block diagram can be seen in Figure 1.

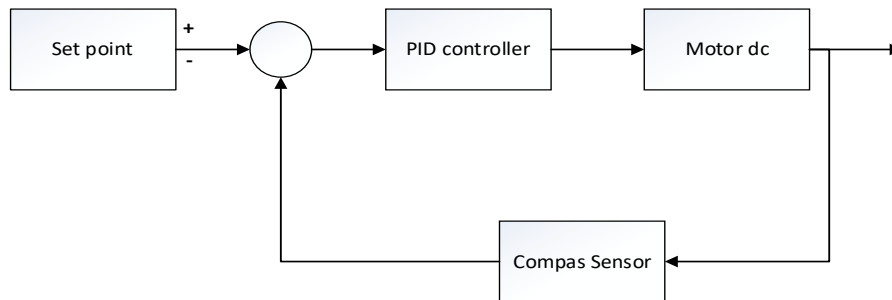


Figure 1. PID Block diagram

2.2 Hardware

As illustrated in Figure 2, the designed system integrates multiple components to achieve real-time data acquisition and control. A camera serves as the primary image capture device, transmitting visual data to the Raspberry Pi for processing. Concurrently, the encoder and compass sensors relay positional and orientation data to the Arduino Mega. The Raspberry Pi processes the visual inputs and synchronizes this information with sensor data received from the Arduino, facilitating cohesive system operation. Processed data and system status are then communicated to the Human Machine Interface (HMI), providing an interactive platform for user engagement. Additionally, the Arduino Mega manages actuators, including motor drivers that control DC motors, which act as the system's main mechanical actuators. This coordinated integration of sensing, processing, and actuation components enables the creation of a responsive and interactive automated system. Figure 3 is a diagram of a block design.

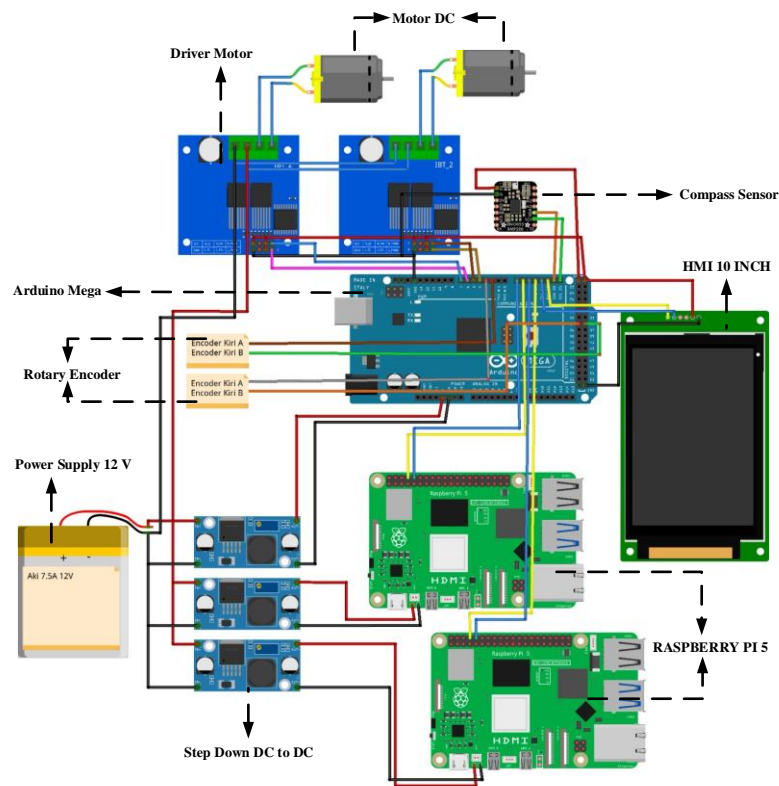


Figure 2. Wiring Diagram

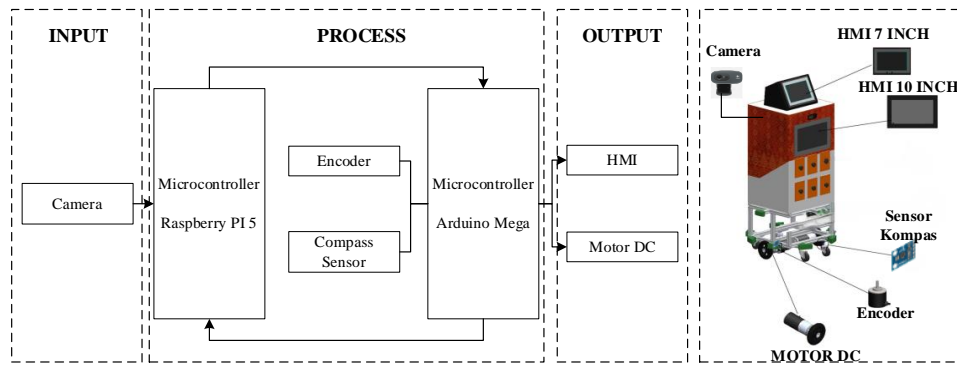


Figure 3. Diagram Block Design

2.3 Detection System Using Yolov5

In this study, the YOLOv5 model was employed due to its suitability for deployment on resource-constrained devices such as the Raspberry Pi [13]. YOLOv5 (You Only Look Once) is a deep learning-based object detection algorithm developed by Ultralytics, representing an evolution of the earlier YOLO series. It is renowned for its capability to perform real-time object detection in images and videos with high speed and accuracy, making it ideal for applications requiring efficient processing on embedded systems. Detection system using YOLOv5 block diagram can be seen in Figure 4.

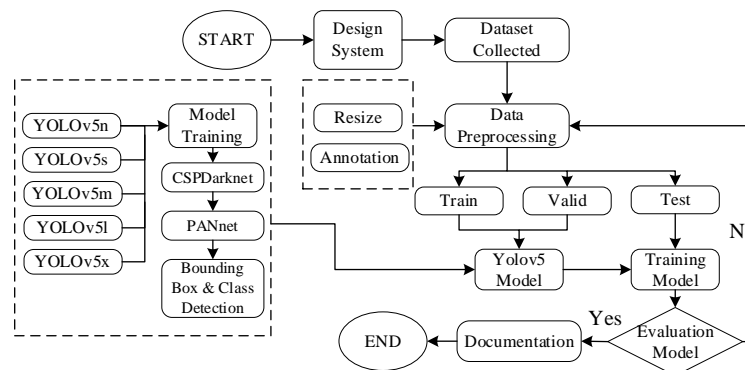


Figure 4. Detection System Using YOLOv5 Block Diagram

2.3.1 Data Collection

YOLOv5 model was trained using a prepared dataset obtained from Roboflow Universe, named Smoking Computer Vision Project [14]. Table 1 shows the detection classes used.

Table 1. Detection Class

Class 0	Class 1	Class 2
Face	Cigarette	Smoking

2.3.2 Data Preprocessing

Once the collected and sorted data are ready, they undergo pre-processing. Pre-processing begins by resizing the images to a standard 640×640 pixels from their original dimensions. Figure 5 shows the YOLOv5 block diagram.

After the resizing process, the next step involves performing static cropping on the images, which means removing unnecessary parts of the image based on predetermined coordinates so that only the relevant area, or Region of Interest (ROI) [15]. Technically, this cropping is carried out by specifying the boundaries of the area to be retained using fixed coordinates (x, y, width, height), ensuring that the resulting image contains only the essential information and reducing noise from irrelevant sections. This process has been shown to improve model accuracy because the model learns only from areas containing the target objects. Once cropping has been applied and the dataset is more focused, the next phase is image annotation. In this phase, each object in the image is labeled, typically using bounding boxes that represent the position and size of the object, or by employing segmentation techniques for more precise edge detection [16]. This annotation process is crucial for producing a high-quality dataset that serves as the foundation for training object detection models.

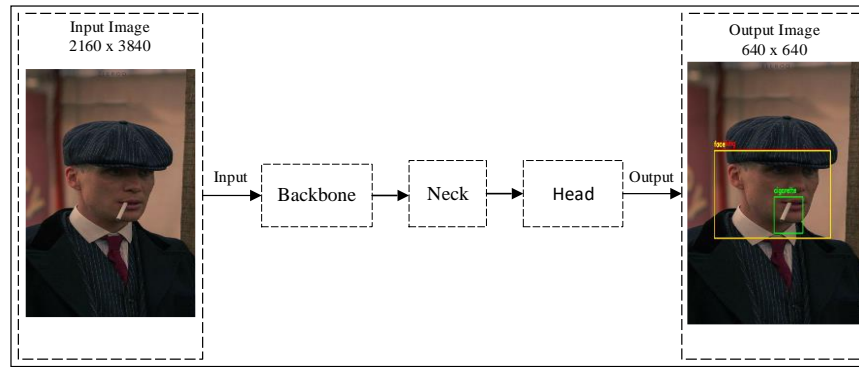


Figure 5. YOLOv5 Block Diagram

2.3.3 Data Split

After the data is collected, it is divided into three categories: training, validation, and testing datasets. The majority of the data, 88%, is assigned to the training set to enable the model to learn effectively from a wide range of examples. Meanwhile, 8% of the data is reserved for validation, allowing for model adjustment and refinement during training. The remaining 4% is reserved for testing, ensuring that the final model's performance is evaluated on unseen data, providing an accurate measure of its ability to generalise. This distribution strategy is designed to optimise model learning and performance evaluation.

2.3.4 Training Model

The YOLOv5 architecture was used to train the model, with the final weights generated from the process considered optimal for image detection during training. Table 2 provides detailed information about the YOLOv5 model training process, including the number of training images, image size, batch size, and number of epochs used.

Table 2 Training Model Details

No	Nama	Image Training	Image size	Batchsize	Epoch
1	Yolov5	2316	640x640	16	300

YOLOv5 is an object detection model known for its efficiency and accuracy. The YOLOv5 architecture comprises three main components (see Figure 6): the Backbone, Neck, and Head. Backbone extracts feature from input images. YOLOv5 utilizes CSPDarknet as its backbone, an extension of Darknet that incorporates a Cross Stage Partial (CSP) mechanism. CSPDarknet iteratively splits and combines gradient information, thereby improving accuracy, feature extraction efficiency, and reducing model size with fewer parameters [17]. The neck is responsible for combining and enriching features from various resolution levels. YOLOv5 uses Path Aggregation Network (PANet) and SPPF (Spatial Pyramid Pooling - Fast) in the neck section. PANet enhances information flow across various backbone layers and facilitates the detection of both small and large objects. SPPF is a faster version of SPP that speeds up the process without reducing output quality [18]. Head is the part that produces the final prediction in the form of bounding boxes, object classes, and confidence scores. In YOLOv5, the head consists of several convolutional layers that produce three outputs at different scales (multi-scale prediction), enabling efficient detection of objects of various sizes. The head structure in YOLOv5 is similar to that used in YOLOv3 and YOLOv4 [19].

2.3.5 Model Testing And Evaluation

In this study, the trained model was tested using new data that had not been used or included in the model training process. This step is crucial for evaluating the model's generalization ability and its effectiveness in accurately detecting objects. The goal is for the model to achieve high accuracy with minimal loss, ensuring reliable detection performance. Figure 7 shows the YOLOv5 architecture used.

One important metric used to evaluate the performance of classification models, especially in the case of object detection or binary classification [20], is

$$\text{Precision} = \frac{TP}{TP+FP} \quad (2)$$

$$\text{Recall} = \frac{TP}{TP+FN} \quad (3)$$

$$mAP = \frac{1}{N} \sum_{i=1}^N AP_i \quad (4)$$

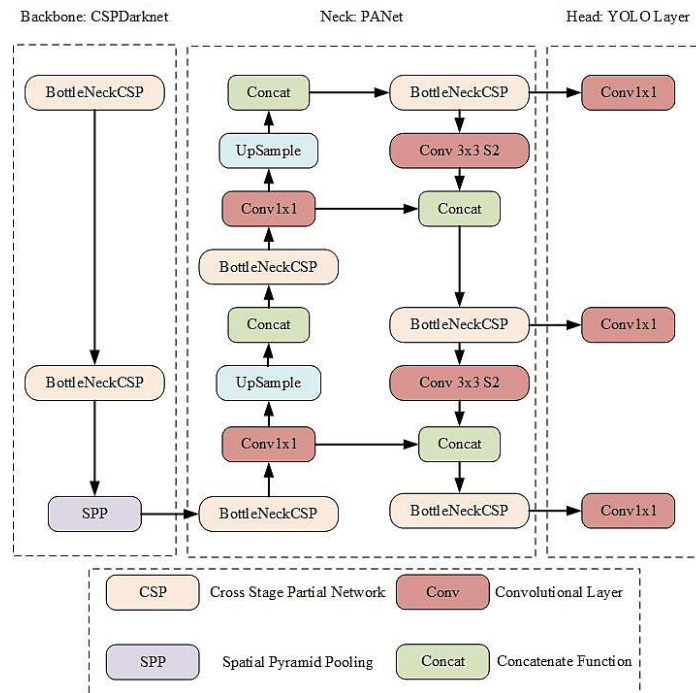


Figure 6. YOLOv5 Architecture

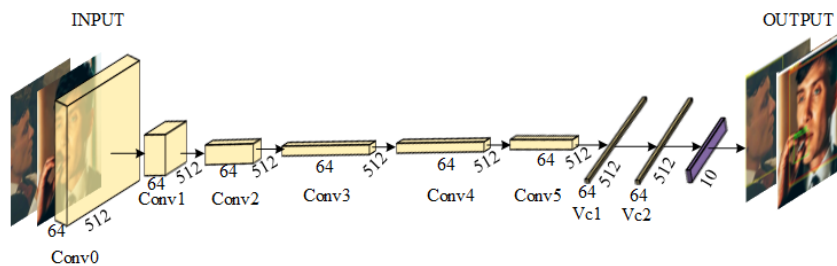


Figure 7. YOLOv5 Architecture Used

3. RESULTS AND ANALYSIS

3.1 Training Data Results

After the training process was complete, the model was evaluated using several performance metrics to assess its effectiveness. The evaluation results showed that the model performed very well in detecting smoking behaviour in no-smoking areas, as indicated by the following values. Training model results can be seen in Table 3.

Table 3. Training Model Results

Model	Precision (%)	Recall (%)	mAP(%)	Size Model (MB)
YOLOv5	98,6%	95,6%	97,6%	14,1 MB

Figure 8 shows the loss and performance curves, indicating a significant decrease in loss during training, both in box loss, object loss, and class loss, which shows that the model successfully minimised detection errors during the training process. Other performance metrics, such as precision, recall, and mAP, showed a steady increase throughout training, with the mAP 0.5 reaching 0.7 in the last epoch. This indicates that the model is becoming increasingly effective at detecting objects with high accuracy during the training process.

Figure 9 shows the model classifies detected objects into three categories: Class 0 represents the face, Class 1 corresponds to cigarettes, and Class 2 indicates the act of smoking. This classification scheme enables the system to not only identify relevant objects but also to determine smoking behavior by

recognizing the interaction between the face and the cigarette, thereby improving the accuracy of smoking violation detection.

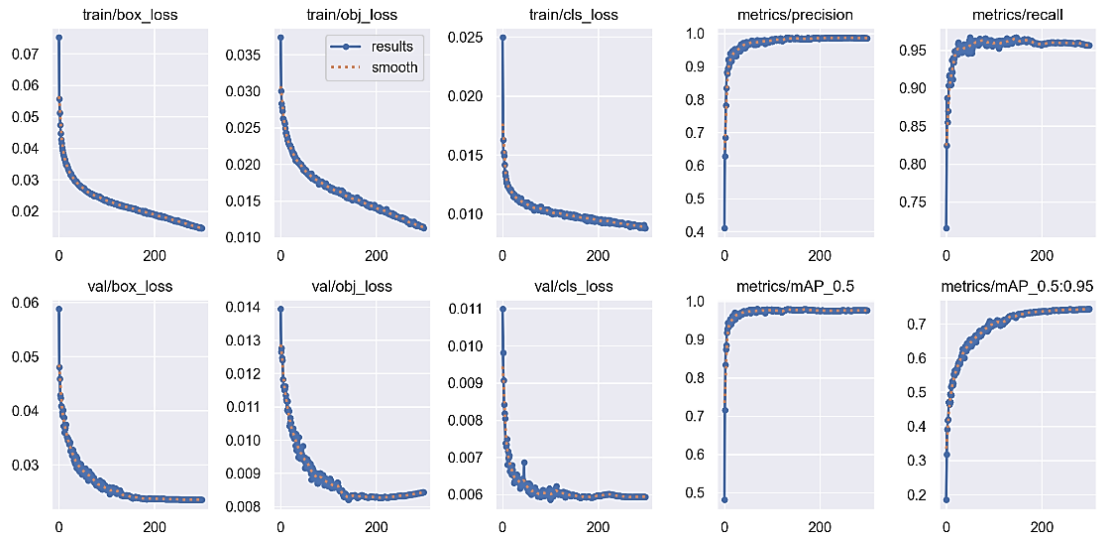


Figure 8. Loss and Performance Curves



Figure 9. Model Detection Results for (a) Face, (b) Face and Cigarette, (c) Person Smoking

3.2 Navigation Data Results

The robot demonstrates effective operation utilizing solely proportional control ($K_p = 4.2$), omitting integral (K_i) and derivative (K_d) components, due to its low-speed movement regulated by a PWM value of 150. At this reduced velocity, the system's inertia and momentum are minimized, diminishing the likelihood of steady-state errors that typically necessitate integral compensation. This simplified control strategy is viable because slower motion inherently reduces overshoot and oscillations, allowing proportional control to maintain stability without additional corrective terms.

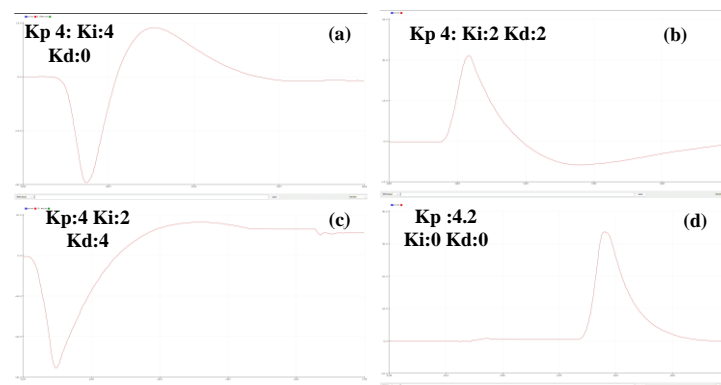


Figure 10. PID error chart

The graphs in Figure 10 show the system's response under different PID (Proportional-Integral-Derivative) control parameters. Graph (a), with $K_p = 4$, $K_i = 4$, and $K_d = 0$, exhibits slow stabilization and significant oscillations due to the absence of derivative action ($K_d = 0$), which fails to effectively dampen the overshoot. In graph (b), with $K_p = 4$, $K_i = 2$, and $K_d = 2$, the response is faster and more stable, with reduced

oscillations thanks to the inclusion of derivative action. Graph (c), with $K_p = 4$, $K_i = 2$, and $K_d = 4$, offers the smoothest and most stable response with minimal overshoot, as the higher derivative action ($K_d = 4$) provides better damping, though it slightly slows the rise time. Finally, graph (d), with $K_p = 4.2$, $K_i = 0$, and $K_d = 0$, achieves the fastest rise to the target but overshoots significantly and oscillates due to the absence of both integral and derivative control. Each graph demonstrates the balance between fast response and stability based on the PID parameters.

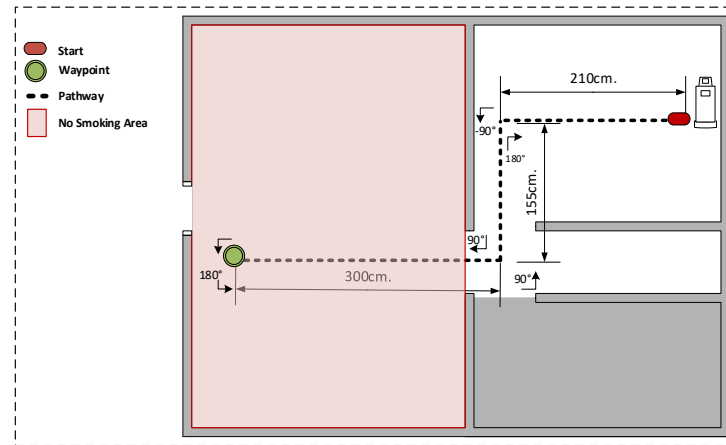


Figure 11. Mapping Robot

Figure 11 demonstrates the navigation performance of the robotic system on a test track comprising straight segments and angular maneuvers, including 90° turns and 180° rotations. Using fixed PID control parameters ($K_p = 4.2$; $K_i = 0$; $K_d = 0$) the system maintained directional stability with minimal heading deviations. Across all path segments, the heading error remained between 0% and 2%, with near-perfect alignment ($< 0.5\%$) observed during straight-line traversal. Despite these transient delays, the system consistently regained stability within 1.2 seconds, achieving final positional accuracy of (< 1 cm) post-maneuver. These results validate the PID controller's efficacy in balancing precision and adaptability, ensuring reliable navigation across heterogeneous path geometries. Table 4 shows the mapping result.

Table 4. Mapping Result

NO	K_p	K_i	K_d	Heading target($^\circ$)	Heading actual ($^\circ$)	Error %	Distance (CM)	System Response
1	4,2	0	0	0	0	0	210cm	Robot maintains its position on the path and continues moving forward smoothly.
2	4,2	0	0	-90	-89,5	0,5	155cm	The robot steadily moves to the left, although at a slow pace.
3	4,2	0	0	90	89,7	0,3	300cm	The robot moves steadily to the right.
4	4,2	0	0	180	178	2	300cm	The robot executes a 180-degree turn steadily, with a slightly delayed response.
5	4,2	0	0	90	89,8	0,2	155cm	The robot moves to the right with steady motion and a prompt response.
6	4,2	0	0	180	178	2	210cm	The robot returns to the home position and moves steadily.

3.3 Object Detection Results

Table 5 shows the data analysis of object detection in this study, which involved evaluating the performance of the YOLOv5-based system in detecting smoking behavior under varying conditions. Testing was conducted across different distances, ranging from 50 cm to 3 meters, and under varying light intensities, measured as flux levels of 46, 90, and 151 lux.

Table 5. Smoking Detection Results.

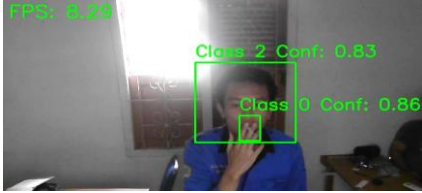
No	Distance	Intensity (Flux)	Confidence score (%)	Fps Average
1	50 cm	46	89 %	
2	100 cm	46	88 %	

No	Distance	Intensity (Flux)	Confidence score (%)	Fps Average
3	150 cm	90	90 %	8 FPS
4		151	92 %	
5		46	87 %	
6		90	88 %	
7		151	88 %	
8	200 cm	46	-	
9		90	86 %	
10		151	88 %	
11	250 cm	90	-	
12		151	87 %	
13	300 cm	151	-	

3.4 Performance Results Of Robot-Based Object Detection

The camera images in Table 6 illustrate the object detection process using YOLOv5, which identifies three classes: class 0 for cigarettes, class 1 for faces, and class 2 for people smoking. Each detection is marked with a green box and a confidence score that indicates the system's confidence score for the detection results in each class. The system is capable of detecting between cigarette objects, faces, and smoking behaviour simultaneously within a single frame, displayed in real-time, with the FPS value also shown in the image.

Table 6. Smoking Detection Results on Robots

No	Camera Results	Description
1.		Test results show a confidence score of 0.94 at a distance of 50 cm with low flux.
2.		Test results show a confidence score of 0.83 at a distance of 100 cm with low flux.
3.		Test results show a confidence score of 0.91 at a distance of 100 cm with high flux.
4.		The test results showed a confidence score of 0.91 at a distance of 150 cm with high flux
5.		Test results show a confidence score of 0.89 at a distance of 250 cm with high flux.

4. CONCLUSION

This study presents an autonomous robot that utilizes YOLOv5 and PID control for detecting smoking violations in restricted areas, achieving a high detection accuracy of 87% with a confidence score at a distance of 250 cm, while operating efficiently on resource-limited devices such as the Raspberry Pi. The robot's navigation system demonstrated precise movement with minimal error, showing an error margin of ± 5 cm over a distance of 2 meters, validating its effectiveness in dynamic and real-time environments for enforcing smoke-free zone regulations.

REFERENCES

- [1] H. Qudus and E. N. Hadi, "Overview of the Implementation of the No Smoking Area (KTR) Policy in the Indonesian Campus Environment: Literature Review," *J. Soc. Res.*, vol. 2, no. 6, pp. 1916–1928, 2023, doi: 10.55324/josr.v2i6.941.
- [2] W. Sulistiadi, M. Veruswati, A. Asyary, M. H. Herawati, R. A. Wulandari, and B. Haryanto, "Smoke-free zone in indonesia: Who is doing what now," *Open Access Maced. J. Med. Sci.*, vol. 8, no. E, pp. 322–324, 2020, doi: 10.3889/oamjms.2020.4091.
- [3] A. M. Fathoni, E. Zuliarso, and U. S. Semarang, "Implementation Of Yolov5 Method In The Cigarette Detection," vol. 7, pp. 1449–1454, 2024.
- [4] L. Arief, A. Z. Tantowi, N. P. Novani, and T. A. Sundara, "Implementation of YOLO and smoke sensor for automating public service announcement of cigarette's hazard in public facilities," *2020 Int. Conf. Inf. Technol. Syst. Innov. ICITSI 2020 - Proc.*, pp. 101–107, 2020, doi: 10.1109/ICITSI50517.2020.9264972.
- [5] A. N. Albab and E. Rahmawati, "Rancang Bangun Sistem Navigasi Mobile Robot Berbasis Sensor Rotary Encoder Menggunakan Metode Odometri," *J. Inov. Fis. Indones.*, vol. 08, no. 2017, pp. 23–27, 2019.
- [6] J. Redmon, S. Divvala, R. Girshick, and A. Farhadi, "You only look once: Unified, real-time object detection," *Proc. IEEE Comput. Soc. Conf. Comput. Vis. Pattern Recognit.*, vol. 2016-Decem, pp. 779–788, 2016, doi: 10.1109/CVPR.2016.91.
- [7] M. Aditya, P. R. Gudpati, K. S. S. Reddy, P. shu, and R. Karampudi, "Smoking Detection using Deep Learning," *Int. J. Comput. Trends Technol.*, vol. 71, no. 02, pp. 8–14, 2023, doi: 10.14445/22312803/ijctt-v71i2p102.
- [8] A. Pundhir, D. Verma, P. Kumar, and B. Raman, "Region Extraction Based Approach for Cigarette Usage Classification Using Deep Learning," *Commun. Comput. Inf. Sci.*, vol. 1568 CCIS, pp. 378–390, 2022, doi: 10.1007/978-3-031-11349-9_33.
- [9] I. Sayekti, B. Supriyo, S. Warjono, S. B. Kuntardjo, and V. S. Kartika, "Rancang Bangun Sensor Kompas Sebagai Pendeteksi Sudut Orientasi Robot Beroda," *J. Elkolind*, vol. 8, no. 3, pp. 397–405, 2022, doi: 10.33795/elkolind.v8i3/259.
- [10] S. Muslimin, E. Prihatini, N. L. Husni, and S. Pebrian, Development Of a Waypoint Navigation System For Rvm Robots Using Path Planning Algorithms Waypoint-Based Path Planning Method. Atlantis Press International BV, 2025. doi: 10.2991/978-94-6463-678-9.
- [11] M. R. Sagita, A. Ma, C. Rekik, W. Caesarendra, and R. Majdoubi, "Motion System of a Four-Wheeled Robot Using a PID Controller Based on MPU and Rotary Encoder Sensors," vol. 2, no. 2, 2024, doi: 10.59247/csol.v2i2.150.
- [12] A. R. Putri, P. Nurrahayu, and A. Anas, "Robot Navigation Control System Using Hmc5883L," *JAREE-Journal Adv. Res. Electr. Eng.*, vol. 3, no. 1, pp. 61–66, 2019.
- [13] M. Wang, D. Qu, Z. Wu, A. Li, N. Wang, and X. Zhang, "Application of Traffic Cone Target Detection Algorithm Based on Improved YOLOv5," *Sensors*, vol. 24, no. 22, 2024, doi: 10.3390/s24227190.
- [14] S. System, "Smoking Dataset," Apr. 2025, Roboflow. [Online]. Available: <https://universe.roboflow.com/survalince-system/smoking-znv6l>
- [15] E. Karantoumanis, V. Balafas, M. Louta, and N. Ploskas, "Computational comparison of image preprocessing techniques for plant diseases detection," *7th South-East Eur. Des. Autom. Comput. Eng. Comput. Networks Soc. Media Conf. SEEDA-CECNSM 2022*, pp. 8–12, 2022, doi: 10.1109/SEEDA-CECNSM57760.2022.9932972.
- [16] S. S. Killikatt, A. Patil, S. Pharakate, S. Koli, S. Wankhade, and M. Patil, "Object Detection and Image Annotation Using Deep Learning," *Int. Res. J. Mod. Eng. Technol. Sci.*, no. 06, pp. 1598–1607, 2023, doi: 10.56726/irjmet41723.
- [17] M. H. Ashar and D. Suarna, "KLIK: Kajian Ilmiah Informatika dan Komputer Implementasi Algoritma YOLOv5 dalam Mendeteksi Penggunaan Masker Pada Kantor Biro Umum Gubernur Sulawesi Barat," *Media Online*, vol. 3, no. 3, pp. 298–302, 2022, [Online]. Available: <https://djournals.com/klik>
- [18] R. A. Setiawan and A. Setyanto, "Evaluasi Trade-off Akurasi dan Kecepatan YOLOv5 dalam Deteksi Kebakaran pada Edge Devices," vol. 5, no. 11, pp. 4647–4655, 2024.
- [19] W. W. Sakti et al., "SKYHAWK: Jurnal Aviati Indonesia Pengembangan Sistem Deteksi Otomatis FOD dengan YOLOv5 di Lingkungan Landasan Bandara," vol. 3, no. 2, 2023, [Online]. Available: <http://ejournal.icpa-banyuwangi.ac.id/index.php/skyhawk>
- [20] M. Dafa Maulana, "Evaluasi Kinerja YOLOv8 dalam Identifikasi Kesegaran Ikan dengan Metode Deteksi Objek," vol. 11, no. 4, pp. 2864–2869, 2024.

BIBLIOGRAPHY OF AUTHORS

Dr. Selamat Muslimin, S.T., M.Kom, is an experienced electrical engineer with a strong background in teaching, research and professional training. He has a proven track record in the field and has contributed significantly to various projects and publications.



Muhammad Andaru Megaarta, a student at the Department of Electrical Engineering, Politeknik Negeri Sriwijaya. Active as a student.



Rayhan Triandika, a student at the Department of Electrical Engineering, Politeknik Negeri Sriwijaya. Active as a student.